1998 ICPP&25th EPS Conf. on Contr. Fusion and Plasma Physics, Praha, 29 June - 3 July. ECA Vol. 22C (1998) 798-801.

Active Control of MHD Modes in a Tokamak*

G. A. Navratil, J. Bialek, A. H. Boozer, C. Cates, M. E. Mauel,
D. Maurer, D. Nadle, and E. Taylor
Department of Applied Physics, Columbia University, New Your, NY 10027 USA
W. A. Reass and G. A. Wurden
Los Alamos National Laboratory, Los Alamos , NM 87545 USA

I. INTRODUCTION

Economically attractive fusion power-plant designs based on advanced tokamak physics emphasize a combination of high beta with a large fraction of well aligned non-inductive bootstrap current to permit economic steady-state operation. However, high beta plasmas with well aligned bootstrap current require operation at levels of $\beta_N = 10^{-8}\ \beta aB/I_p$ well above the beta limit for the low-n ideal kink mode.[1,2] While the n=1 ideal kink no-wall β-limit, β_{nw}, has been modestly exceeded ($\beta \leq 1.4\beta_{nw}$) in DIII-D[3] and HBT-EP[4] in wall-stabilized plasmas, the higher β-limits predicted for a perfectly conducting wall ($\beta \sim 2$ to $3\beta_{nw}$)[5] have not yet been achieved due to the onset of slowly growing resistive modes. This paper reports experiments in HBT-EP to actively control the most important slowly growing modes: the 2/1 tearing mode and the resistive wall mode (RWM).

II. MODE CONTROL SYSTEMS AND BASIC PARAMETERS OF HBT-EP

The approach to mode control in HBT-EP consists of a combination of active and passive stabilization techniques. A 10 segment, adjustable conducting wall is used to provide passive stabilization of the low-n ideal kink mode. Active control of the residual slower growing 2/1 tearing modes is effected by applications of rotating helical magnetic field perturbations generated by highly modular saddle coils external to the vacuum vessel. This configuration is shown schematically in Fig. 1. The toroidal plasma has an aspect ratio, R/a = 6 with R = 0.92 meters. The passive stabilizing conducting wall consists of ten, 1 cm thick aluminum segments, each of which covers 26° of toroidal angle. These wall segments can be varied in radial position to study the effect of wall proximity on kink mode stabilization and these results have been published previously.[2,6] In the experiments reported in this paper on active mode control, the wall segments were positioned less than 10% of the plasma minor radius from the plasma edge for maximum passive stabilization of the ideal time scale modes.

At four of the 10° wide gaps in the conducting wall segments are located m=2 saddle coils. Each of these saddle coils is 6° wide in toroidal angle and positioned in poloidal angle to couple optimally to an m=2, n=1 helical field. The saddle coils project a radial field into the plasma through 5° wide quartz toroidal gaps that allow efficient penetration of magnetic perturbations with frequencies up to 20 kHz. This highly modular configuration only covers about 3% of the toroidal surface surrounding the plasma.

Two of these saddle coils are connected in series and driven with a 10 MW linear amplifier to provide a $\sin(\omega t+\delta)$ response field and the other two coils are connected in series and driven with an independent 10MW linear amplifier to provide a $\cos(\omega t+\delta)$ response field; together these coils provide a 2-phase, quadrature winding to producing a rotating magnetic

perturbation. The 10 MW linear amplifiers used in these experiments have a bandwidth greater than 25 kHz and can deliver ±600 Amperes through each of the 9-turn saddle coils. The phase and amplitude information from the rotating 2/1 island structure in the plasma is obtained from a set of sin2θ and cos2θ Rogowski coils which are physically remote (as shown in Fig 1) from the saddle coil response fields and have very low direct pick-up.

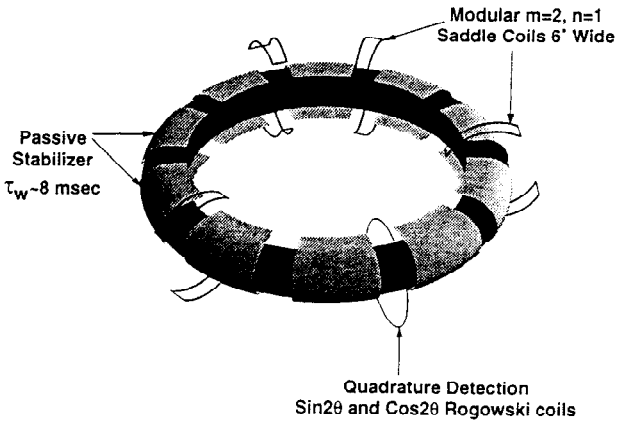

Figure 1. Schematic of the HBT-EP control coil configuration showing ten 26° wide conducting wall segments with 6° wide m=2 saddle coils located at 4 of the 10° wide gaps in the conducting wall segments. A sin2θ and cos2θ Rogowski coil quadrature detector is located to be physically remote from the saddle coils.

III. CONTROL OF 2/1 MAGNETIC ISLANDS

By applying a rotating external 2/1 field which is maintained in a stabilizing phase relation with the mode, we have used a closed loop system to carry out active feedback suppression of the 2/1 island amplitude. The quadrature detection scheme measures a sin2θ and cos2θ signal as a phase and amplitude reference for closed loop active feedback. These sin2θ and cos2θ signals are digitized at a 100 kHz rate and processed by a digital signal processor to generate a phase shifted waveform that drives the high power amplifiers and applies a 2/1 rotating applied field with a predetermined phase shift with respect to the rotating islands. The feedback control algorithm implements a simple rotation matrix which maintains a constant phase angle, δ, between the detected mode phase and applied external rotating field.

We can model[7] the expected equilibrium response of the 2/1 islands assuming that $\Omega\tau_{wall} >> 1$ we solve the following coupled non-linear equations for the expected mode amplitude and frequency as a function of phase angle and closed loop system gain, G.

$$0 = g_1\left(1 - \sqrt{b}\right)\sqrt{b} + g_2 G\cos(\delta)\sqrt{b} - g_3\frac{(\Omega - 1)^2}{b} \qquad (1)$$

$$0 = -h_1(\Omega - 1) + h_2 G\sin(\delta)b - \frac{h_3 b^2}{\Omega\tau_{wall}} \qquad (2)$$

where, g_1, g_2, g_3, h_1, and h_2 are constants. With W_{sat} defined as the saturated island width, $b \equiv (W/W_{sat})^2$; and $\Omega \equiv \omega/\omega_o$, where ω_o is the natural island rotation frequency. This model indicates reduced amplitude (stabilizing) for $\delta = 0°$ and larger amplitude for $\delta = 180°$.

Closed loop experiments were carried out for $\delta = 0°$ and 180° on a single discharge with the stabilizing phase angle applied for 1 msec followed by the destabilizing phase angle applied for the following 1 msec. These results are shown in Fig. 2 showing the time history of δ, the amplitude of the sine and cosine phase of the 2/1 islands, and the frequency of the

island rotation. During the 1 msec application of the stabilizing phase angle, the frequency is observed to rise from about 7 kHz to 10 kHz with a relatively constant amplitude. After the transition to the destabilizing phase angle, the mode amplitude is observed to grow larger and the frequency of the mode is observed to decline from 10 kHz to 7 kHz in agreement with the expectations of the equilibrium model of Eqs. (1) and (2). If the data is averaged over 0.1 msec intervals and plotted against the predictions of the model, we find reasonably good agreement as also shown in Fig. 2.

A similar experiment was carried out for phase angles δ = 270° and 90° where we expect a frequency decrease and frequency increase. The results are shown in Fig. 3. During the initial application of the frequency decrease phase angle, we see the frequency maintained at about 7 kHz. After the transition to the frequency increase phase angle, the island rotation frequency is observed to increase to about 9 kHz over 1 msec. These results are also plotted averaged over 0.1 msec intervals against the model predictions showing good agreement.

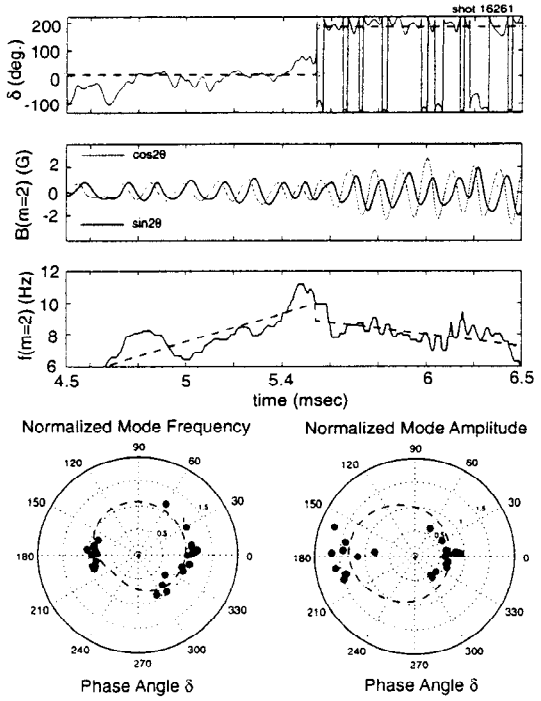

Figure 2. Application of stabilizing (0°) phase and destabilizing (180°) phase each for 1 msec compared with the results of the model equations.

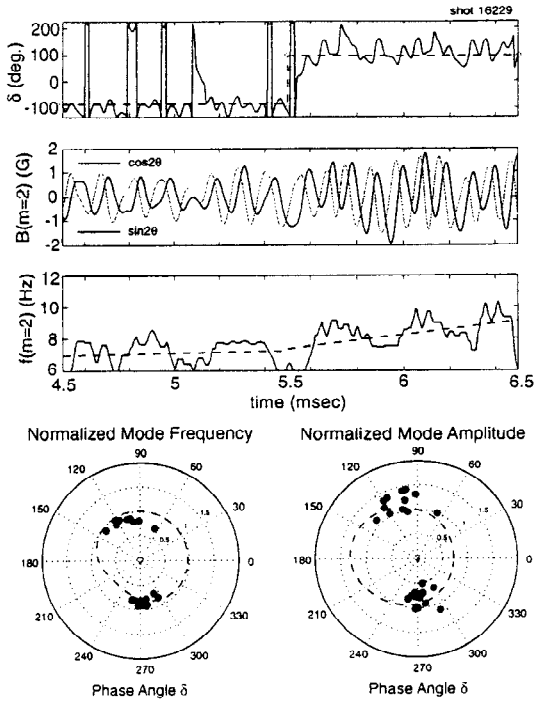

Figure 3. Application of frequency downshift (270°) phase and frequency upshift (90°) phase compared with the results of the model equations.

IV. CONTROL OF THE RESISTIVE WALL MODE

Several schemes have been proposed for control of the slower growing RWM using active feedback control by external coils in conjunction with a passive resistive wall stabilizer. For the "smart shell" originally proposed by Bishop[8] a network of flux sensor loops is mounted on the surface of the resistive stabilizing wall, with an array of current-carrying response coils located near the wall powered by an amplifier system. The flux sensor loops sense the radial magnetic field, B_r, soaking through the resistive wall and feedback control is used to apply a correction field which maintains very closely a net zero B_r through the resistive wall simulating the stabilizing response of a perfectly conducting wall.

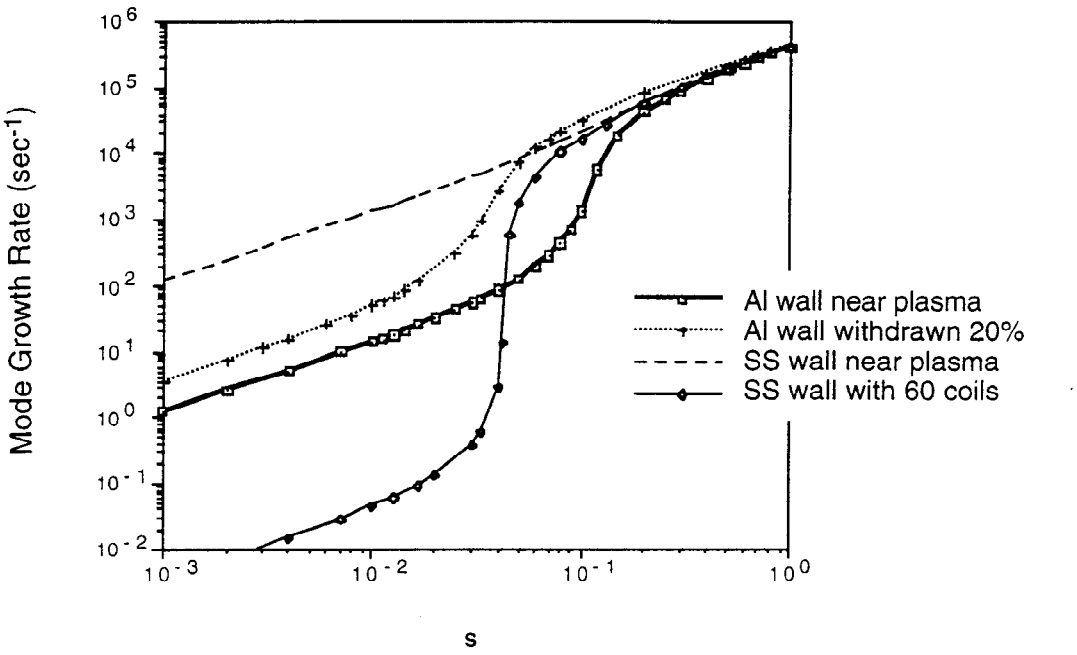

Figure 4. Computed growth rate of 3/1 kink in for HBT-EP as wall conditions and mode 'drive', s, are varied.

To provide a general tool for the analysis of such active control schemes, we have developed a 3D active mode control model code based on the SPARK finite element electromagnetic code. This has been used to model the control geometry of HBT-EP as shown in Fig. 4, where **s** is the instability "strength" which is related to βN and varies between 0 and about 1. For the open square symbol curve at $s \geq 0.1$ in Fig. 4, the large change in growth rate is seen marking the transition from the RWM branch to the ideal mode branch of the dispersion relation with the thick aluminum wall of HBT very close to the plasma. This corresponds to a β_N of about 3. For the curve marked by crosses, this maps the dispersion relation when the thick aluminum wall is withdrawn to 20% of the minor radius of the plasma and the plasma is observed to become ideally unstable at $\beta_N \sim 1.9$. The curve marked with an open diamond shows the effect on stability from an ideal smart shell using 60 discrete coils behind a very resistive stainless steel wall ($\tau_{wall} \leq 300$ μsec). The transition from growth rates of 1 sec^{-1} to 10^4 sec^{-1} (*i.e.* stable to unstable) occur for a larger value of s, and hence we expect to achieve a higher value of beta above the no-wall beta limit when this system is installed on HBT-EP.

---

* Supported by US DOE Grant DE-FG02-86ER53222.

[1] C. Kessel, J. Manickam, G. Rewoldt, and W. Tang, *Phys. Rev. Lett.* **72**, 1212 (1994); J. Manickam, M. S. Chance, S. C. Jardin, *et al.*, *Phys. Plasmas* **1**, 1601 (1994).

[2] A. Turnbull, T. S. Taylor, Y. R. Lin-Liu, and H. St. John, *Phys. Rev. Lett.* **74**, 718 (1995).

[3] T. Taylor, E. J. Strait, L.L. Lao, M. Mauel, *et al.*, *Phys. Plasmas* **2** (1995) 2390.

[4] T. H. Ivers, E. Eisner, A. Garofalo, *et al*, *Physics of Plasmas* **3**, (1996) 1926.

[5] Kessel, J. Manickam, G. Rewoldt, and W. Tang, *Phys Rev Lett* **72** (1994) 1212.

[6] Andrea Garofalo, E. Eisner, T. H. Ivers, *et al.*, *Nucl. Fusion* **38** (1998) to be published.

[7] G. A. Navratil, C. Cates, M. E. Mauel, *et al.*, *Phys. Plasmas* **5**, 1855 (1998).

[8] C. M. Bishop, *Plasma Phys. Contr. Fusion* **31**, 1179 (1989).